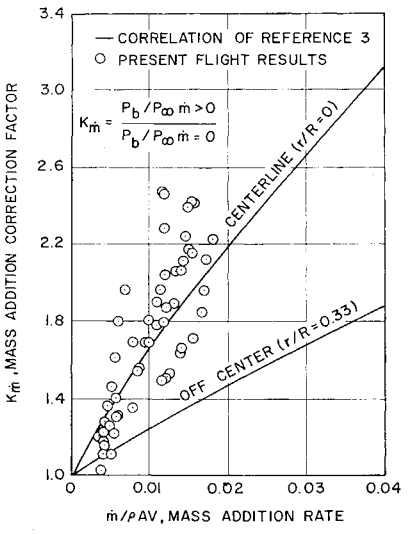


**Fig. 6 Mass addition correlation.**

corresponding with the flights having high base pressures and low rates $\dot{m}/\rho AV \approx 0.007$ corresponding with flights having low base pressures.

### IV. Flow Mechanism Hypothesis

The following hypothesis[3,4] is postulated as the primary mechanism which accounts for the increase in base pressure with increasing mass addition. Mass addition tends to thicken the boundary layer and especially the laminar sublayer. The large laminar sublayer can result in a pseudo-laminar base flow region. The thicker boundary layer, which includes the mass flow from the ablating process, is swept into the wake region and tends to enlarge the neck of the wake and force it downstream, thus changing (decreasing) the wake expansion angle, as shown in Fig. 3. The smaller expansion angle is similar to what would be expected in laminar flow, and results in a higher base pressure ratio. This phenomena is illustrated in Figs. 4 and 5 and is based on the results of ground tests on a nonablating body.[2] The flow turning angle ($\Delta\theta$) can be seen to be less in laminar flow than turbulent flow (Fig. 4), whereas the base pressure is higher in laminar flow than turbulent flow (Fig. 5).

### V. Base Pressure Mass Addition Correlation

The flight data from the seven flights correlated nicely when the ratio of base pressure with mass addition to base pressure with zero mass addition was plotted as a function of $\dot{m}/\rho AV$ (Fig. 6). Since all of the flights considered had ablative heat shields, the zero mass addition base pressure levels were obtained from the prediction technique of Ref. 3 for $\dot{m}/\rho AV = 0$. The pressure data are in qualitative agreement with the empirical correlation of Ref. 3 and show that base pressure ratio has a near linear type relationship with mass addition rate. This trend of increasing base pressure with increasing mass addition rate has also been observed in the ground test data of Refs. 5 and 6. The correlation of Ref. 3 indicates that a radial pressure gradient is present on the base due to mass addition effects. The present data were not sufficient to verify this trend. It is suspected but not verified that the correlation of the present data is unique to the mass addition distribution for these flight vehicles. Flight vehicles having different mass addition distributions (but the same approximate rates $\dot{m}/\rho AV \approx 0.007$ to 0.014) would have differences in the local conditions preceding the base. This may explain why the present data are in qualitative rather than quantative agreement with the correlation of Ref. 3.

### References

[1] Whitfield, J. D. and Potter, J. L., "On Base Pressures at High Reynolds Numbers at Hypersonic Mach Numbers," TN-60-61, March 1960, Arnold Engineering Development Center, Tullahoma, Tenn.

[2] Cassanto, J. M., "Base Pressure Measurements on Free-flight and Sting Supported Modes at $M = 4$," *AIAA Journal*, Vol. 6, No. 7, July 1968, pp. 1411–1414.

[3] Cassanto, J. M. and Storer, E. M., "A Revised Technique for Predicting the Base Pressure of Sphere Cone Configurations in Turbulent Flow Including Mass Addition Effects," Aerodynamic Fundamentals Memo ALFM 68-41, Oct. 1968, General Electric Co.

[4] Cassanto J. M. and Mendelson, R. S., "Local Flow Effects on Base Pressure," *AIAA Journal*, Vol. 6, No. 6, June 1968, pp. 1182–1185.

[5] Fox, J., Zakkay, V., and Sinah, R., "A Review of Some Problems in Turbulent Mixing," Rept. NYU-AA-66-63, Sept. 1966, New York Univ.

[6] Lewis, J. E. and Chapkis, R. L., "Mean Properties of the Turbulent Near Wake of a Slender Body With or Without Base Injection," *AIAA Journal*, Vol. 7, No. 5, May 1969, pp. 835–841.

## Mean Density and Temperature Data in Wakes of Hypersonic Spheres

J. G. G. Dionne* and L. Tardif*
*Defence Research Establishment Valcartier, Quebec, Canada*

THE successful use of electron beam fluorescence probes in the study of mass density and temperature in shock tubes and shock tunnels[1–3] has led experimenters to use this probing system to study wakes of hypersonic projectiles.[4,5] The superiority of such a system is essentially its minimum interference with the gas flow, and its most serious drawback is its limited effectiveness at ambient pressures above 10 torr.

The electron beam generator itself and the optical system used to measure the induced fluorescence have been detailed elsewhere[5]; the main characteristics are a 2 milliamperes beam capability at 100 KV for the generator and a large-aperture optical system. The field of view is defined geometrically by a slit, and spectrally by an interference filter. The bulk of emission induced by the electrons in nitrogen or air is represented by the $N_2$ second positive and by the $N_2$ first negative systems[6]; for both intensity and linearity reasons, the latter is preferred at pressures below one torr, and the former, at pressures above three torr. Muntz[1] has studied the excitation and emission processes for the first negative system, and Camac[7] has reported that the emission of the second positive system is produced not by the primary electrons but by the secondary electrons formed by the primary beam. The emission will thus be produced around the primary beam within the range of the secondary electrons. As the pressure increases, the effective range of the secondary electrons decreases, while the primary beam spreads out. Measurements have shown that the primary beam spreading increases rapidly with the pressure-distance product. Also, the effective beam width is larger at 3371 Å $N_2$[2P(0,0)] than at 3914 Å $N_2^+$[1N(0,0)], particularly at pressures below one torr, as the secondary electron range increases with decreasing pressure while a negligible beam spreading of the primary beam is experienced.

Received February 9, 1970; revision received May 15, 1970. The authors are indebted to members of the Defence Research Establishment Valcartier (DREV), Aerophysics Division, for their support. The work is part of a joint DREV-Advanced Research Projects Agency (ARPA) program for investigation of the hypersonic turbulent wake under ARPA Order 133.

* Defense Scientific Service Officer.

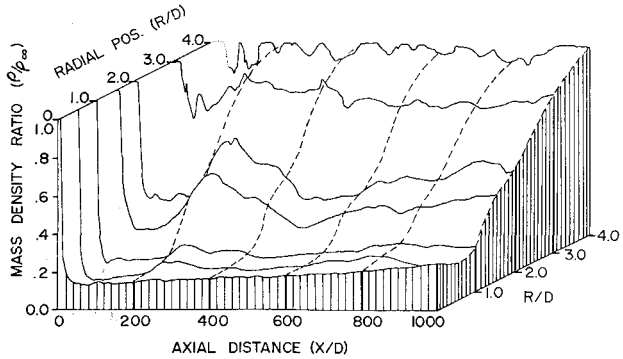


**Fig. 1 Mass density distribution in a laminar wake (proj: 2.7 in. diam ti. sphere; $P_\infty$ = 1 torr of $N_2$; $V_\infty$: 15,000 fps).**

### Signal Analysis

When used at a low enough pressure to preclude nonradiative de-excitation processes and to minimize beam attenuation and spreading, the fluorescence emission observed is proportional either to the mass density or to the square of its value. The latter relation applies to the second positive system when the field of view is smaller than the range of the secondary electrons and the former to both systems in all other cases. As pressure increases the emission intensity function is changed and the relation between fluorescence emission and mass density becomes more complex. This can be described as

$$S(y) = k_0 i(y) W(y) C(\rho) \qquad (1)$$

where $S$, represents the measured signal; $i$, the beam current; $W$, the beam width at a detector position $y$, from the beam origin; $k_0$ is a proportionality constant taking into account the various parameters such as amplifier gain, detector sensitivity and collecting optics properties. The function $C(\rho)$ represents the calibration function relating the fluorescence to the mass density. Since the beam current is partially attenuated, its value at the detector is determined using an exponential attenuation function experimentally defined. Bearing in mind the relatively high rectangular field of view (1.2 mm × 12 mm), the beam spreading can be neglected as the beam is always smaller than the detector aperture. Similarly the quasi-linear relation for the calibration function reported before[4] can be retained, as the range of the secondary electrons produced is always smaller than the height of the field of view at the pressures of interest here.

### Experimental Wake Density

The density measurements have been done in wakes of 2.7 in. diam titanium spheres in nitrogen atmospheres. All

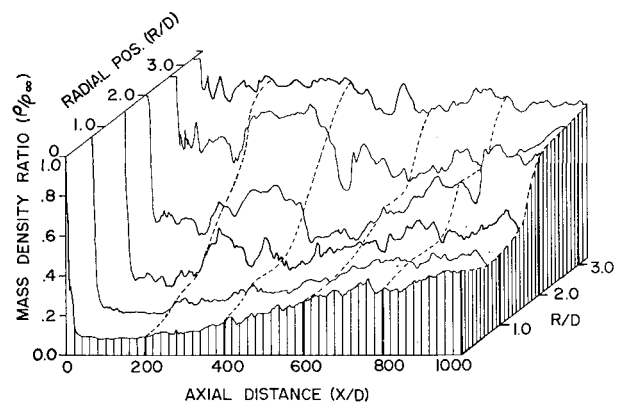


**Fig. 2 Mass density distribution in a turbulent wake (proj: 2.7 in. diam ti. sphere; $P_\infty$: 7.6 torr of $N_2$; $V_\infty$: 15,000 fps).**

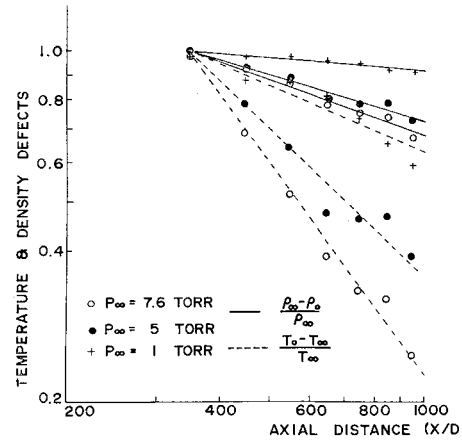


**Fig. 3 Axial density and temperature defects (proj: 2.7 in. diam ti. sphere; $V_\infty$: 15,000 fps; gas: $N_2$).**

spheres were fired at a velocity of 15,000 fps and pressures of 1.0, 5.0, and 7.6 torr were chosen to obtain laminar, transitional, and turbulent wakes. At each pressure, the density data collected at various mean radial distances ($R/D$) from the wake center are averaged. The resulting averages are reproduced in Figs. 1 and 2 for pressures of 1.0 and 7.6 torr.

The laminar wake data (Fig. 1), averaged over four firings, can be used to determine the qualitative features of laminar wake: first, the density is nearly constant or increases slowly at any radial position up to one thousand body diameters; secondly, the low density laminar core is approximately two body diameters in size; thirdly, the level of density fluctuation is low and contains very little high frequency. However the small density fluctuations measured at the outer edge of the wake ($R/D$ = 4) can be associated with some corrugations or instabilities of the wake edge as the maximum density measured is equal to the density outside the wake. Using these criteria, the wake density data represented in Fig. 2 shows a laminar wake core (constant density and diameter) extending up to 200 body diams followed by a turbulent core, characterized by its greater rate of diffusion, its larger amplitude of density fluctuations and its higher frequency content.

On both graphs, the density increase between 200 and 400 body diams is attributed to the interference of the reflected bow shock. Schlieren measurement and wake velocity distribution profiles have shown that the shock disturbance in an unsymmetrical tank geometry causes a lateral movement of the wake, which, in the case of interest here, is measured as a temporary density increase when the wake center is blown outside the flight axis.[8] Moreover, to ensure that the interference does not invalidate the wake data after the shock interaction, wakes of smaller diameter spheres were also measured. In this case the reflected shock interaction was observed at 600 body diams and the density data, up to that position, have confirmed the density measurements reported here.

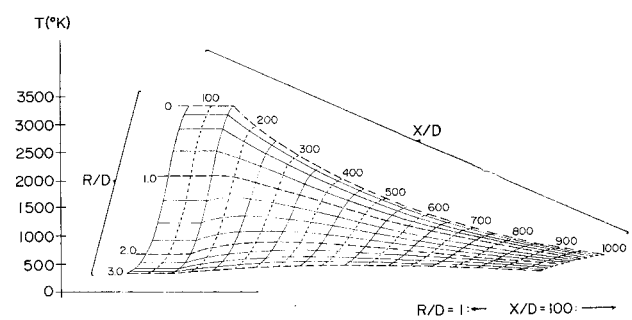


**Fig. 4 Wake temperature inferred from density measurements (proj: 2.7 in. diam ti. sphere; $P_\infty$: 7.6 torr of $N_2$; $V_\infty$: 15,000 fps).**

### Wake Density and Temperature

#### *Axial results*

Of all the laws governing the wakes, the growth law is certainly the best established one. As the wake growth is faster for turbulent than for laminar wakes, the density $[(\rho_\infty - \rho_0)/\rho_\infty]$ and temperature $[(T_0 - T_\infty)/T_\infty]$ defects diffuse or decrease more rapidly in turbulent than in laminar wakes; graphical presentations of this decrease vs downstream distance have been presented by Demetriades.[9] In Fig. 3, the normalized density and temperature defects are given. For the density data, slopes of 0.09, 0.32, and 0.36 are found respectively for 1.0, 5.0, and 7.6 torr, and for the temperature defects, the slopes found are 0.42, 1.00, and 1.46 for 1.0, 5.0, and 7.6 torr. The temperature data given here are obtained by inverting the density data, since, according to Lykoudis,[10] the pressure will be nearly ambient at a downstream distance $X/D$ approximately equal to $M^2/9$; in our case, this distance is 25 $X/D$, so the hypothesis of an isobaric wake is justified. The marked difference between the density and temperature decay rates is to be expected as a result of the form of the equation of state in the hypothesis of an isobaric wake as pointed out by Demetriades.[9]

#### *Radial results*

The radial variation of the density form parameter $[(\rho_\infty - \rho)/(\rho_\infty - \rho_0)]$ can be compared with the density results computed by Wen.[11] As the density distribution is not gaussian while the temperature is, it is more interesting to compute wake temperature from the density data assuming an isobaric wake. All the temperature data so obtained can be fitted by a gaussian distribution which shows good agreement with Wen's results. Moreover all the distributions curves obtained at several distances in the wake can be used to produce a complete map of the average temperature of the wake represented by the carpet plot of Fig. 4. The first part of the wake extending up to 150 body diams is fitted by a gaussian radial distribution and a constant value along the wake axis. Beyond that point, the radial gaussian distribution is retained and the axial data is fitted by an exponential decay of temperature.

### Concluding Remarks

The free flight range facility has shown great potentiality for wake studies behind hypersonic models. However this facility provides data which are often statistically poor because of the limited number of firings observed and of the short observation time available on each firing. This is particularly true for the large size models required to develop a turbulent wake at an ambient pressure not exceeding 10 torr. Evidently our data suffer from this drawback since only 4 firings at 1.0 torr and 7 at 7.6 torr were made available.

### References


[1] Muntz, E. P., "Static Temperature Measurements in a Flowing Gas," *The Physics of Fluids*, Vol. 5, No. 1, Jan. 1962, pp. 80–90.

[2] Muntz, E. P. and Softley, E. S., "A Study of Laminar Near Wakes," *AIAA Journal*, Vol. 4, No. 6, June 1966, pp. 961–968.

[3] Rothe, D. E., "Electron Beam Studies of the Diffusive Separation of Helium-Argon Mixtures," *The Physics of Fluids*, Vol. 9, No. 9, Sept 1966, pp. 1643–1658.

[4] Dionne, J. G. G. et al., "Mass Density Measurements in Hypersonic Wakes," *AGARD Conference Proceedings No. 19, Fluid of Physics of Hypersonic Wakes*, Colorado State Univ., May 1967.

[5] Tardif, L. and Dionne, J. G. G., "Density Distribution in Turbulent and Laminar Wakes," *AIAA Journal*, Vol. 6, No. 10, Oct. 1968, pp. 2027–2029.

[6] Davidson, G. and O'Neill, R., "The Fluorescence of Air and Nitrogen Excited by 50 Kev Electrons," AFCRL-64-466, May 1964, Air Force Cambridge Research Lab, Bedford, Mass.

[7] Camac, M., "Boundary Layer Measurements with an Electron Beam," Research Report 275, 1967, AVCO Everett, Everett, Mass.

[8] Robertson, W. J., "The Effect of Reflected Shock System on Hypersonic Wakes," TN/1846/69, 1969 Defence Research Establishment Valcartier, Quebec, Canada.

[9] Demetriades, A., "Mean-Flow Measurements in an Axisymmetric Compressible Turbulent Wake," *AIAA Journal*, Vol. 6, No. 3, March 1968, pp. 432–439.

[10] Lykoudis, P. S., "A Review of Hypersonic Wake Studies," *AIAA Journal*, Vol. 4, No. 4, April 1966, pp. 577–590.

[11] Wen, K. S., Chen, T., and Lieu, B., "A Theoretical Study of Hypersonic Sphere Wakes in Air and Comparisons with Experiments," AIAA Paper 68-703, Los Angeles, Calif., June 1968.


## Observations of Surface Ablation Patterns in Subliming Materials


A. L. Laganelli* and R. E. Zempel†

*General Electric Company, Valley Forge, Pa.*


### Introduction

THE discovery of surface ablation patterns on ground test models as well as recovered flight vehicles, with the subsequent conjectures explaining the phenomena, has been an item of interest over the past few years. A comprehensive review of the subject matter (up through mid-1968) can be found in a paper by Laganelli and Nestler.[1] Several additional investigations concerning the phenomena consist of the theoretical analyses of Donaldson,[2] Lew and Li,[3] Inger,[4] Tobak,[5] Nachtsheim,[6] Person,[7] and Probstein and Gold[8] as well as the experimental results of Williams.[9]

The present study consisted of investigating surface ablation patterns as developed by natural ablation and by introducing disturbances on the body. The test program was conducted in the NASA Langley 8-Ft High-Temperature Structures Tunnel. The facility provides a nominal free-stream Mach number of 7.4, stagnation temperature up to 3500°R, and stagnation pressure range from 1000 to 2800 psia. The experimental models consisted of sharp-tipped Teflon cones with a base diameter of approximately 30 in. and a half-angle of 36°. The actual test matrix conducted in the Langley facility consisted of many tests whose results would be beyond the scope of this Note. These tests included single and multiple rows and columns of drilled holes and pins at various longitudinal and lateral spacings and depths, random-spaced holes, logarithmic-spaced holes, slots, steps, dissimilar materials, and angle-of-attack effects. Several of the more pertinent features of the tests will be reported, and interested readers can find specific details in Ref. 2. Preliminary tests were made to confirm local pressure predictions and to indicate what test exposure time was required to produce the patterns. The results of these tests are reported in Ref. 1.

### Test Results

Inasmuch as the test time for the Langley facility was limited (30 secs) it was decided to reablate one of the preliminary models (shown in Fig. 1) to simulate longer ablation time. The results of this test are shown in Fig. 2. It is observed that the longer ablation time appeared to produce


Received April 17, 1970; revision received May 27, 1970. The authors wish to acknowledge the U.S. Air Force who sponsored this work under Contract AF-04(694)914. Also, the authors thank D. E. Nestler who supervised much of the work and S. Stadelmeier for his photographic and measurement techniques.



* Research Engineer, Aerothermodynamics Re-entry and Environmental Systems Division. Member AIAA.

† Research Engineer, Aerothermodynamics, Re-entry and Environmental Systems Division.